



Published in final edited form as:

*J Immunol.* 2007 November 1; 179(9): 6246–6254.

## Biomechanical Signals Suppress TAK1 Activation to Inhibit NF- $\kappa$ B Transcriptional Activation in Fibrochondrocytes

Shashi Madhavan<sup>\*</sup>, Mirela Anghelina<sup>\*</sup>, Danen Sjoström<sup>\*</sup>, Anar Dossumbekova<sup>\*</sup>, Denis C. Guttridge<sup>†</sup>, and Sudha Agarwal<sup>\*,‡,2</sup>

<sup>\*</sup>Biomechanics and Tissue Engineering Laboratory, Section of Oral Biology, The Ohio State University, Columbus Ohio 43210

<sup>†</sup>Department of Molecular Virology, Immunology and Medical Genetics, The Ohio State University, Columbus Ohio 43210

<sup>‡</sup>Department of Orthopedics, The Ohio State University, Columbus Ohio 43210

### Abstract

Exercise/joint mobilization is therapeutic for inflammatory joint diseases like rheumatoid and osteoarthritis, but the mechanisms underlying its actions remain poorly understood. We report that biomechanical signals at low/physiological magnitudes are potent inhibitors of inflammation induced by diverse proinflammatory activators like IL-1 $\beta$ , TNF- $\alpha$ , and lipopolysaccharides, in fibrochondrocytes. These signals exert their anti-inflammatory effects by inhibiting phosphorylation of TAK1, a critical point where signals generated by IL-1 $\beta$ , TNF- $\alpha$ , and LPS converge to initiate NF- $\kappa$ B signaling cascade and proinflammatory gene induction. Additionally, biomechanical signals inhibit multiple steps in the IL-1 $\beta$ -induced proinflammatory cascade downstream of I $\kappa$ B kinase activation to regulate I $\kappa$ B $\alpha$  and I $\kappa$ B $\beta$  degradation and synthesis, and promote I $\kappa$ B $\alpha$  shuttling to export nuclear NF- $\kappa$ B and terminate its transcriptional activity. The findings demonstrate that biomechanical forces are but another important signal that uses NF- $\kappa$ B pathway to regulate inflammation by switching the molecular activation of discrete molecules involved in proinflammatory gene transcription.

Arthritic diseases are chronic inflammatory diseases of the joints associated with significant cartilage and bone erosion resulting in compromised joint function. Increased production of cytokines including IL-1 and TNF- $\alpha$  (1, 2) by the synoviocytes and chondrocytes provide evidence for their involvement in the pathogenesis of both, rheumatoid arthritis (RA)<sup>3</sup> and osteoarthritis (OA). These cytokines up-regulate transcription of proinflammatory genes such as inducible NO synthase (NOS2A), cyclooxygenase-2 (COX-2), matrix metalloproteinases (MMPs), IL-1 $\beta$ , and TNF- $\alpha$  to initiate cartilage destruction and amplify

<sup>2</sup>Address correspondence and reprint requests to Dr. Sudha Agarwal, The Ohio State University, 4171 Postle Hall, 305 West 12th Avenue, Columbus, OH 43210. Agarwal.61@osu.edu.

#### Disclosures

The authors have no financial conflict of interest.

<sup>3</sup>Abbreviations used in this paper: RA, rheumatoid arthritis; OA, osteoarthritis; COX, cyclooxygenase; MMP, matrix metalloproteinase; FC, fibrochondrocyte; IKK, I $\kappa$ B kinase; TMJ, temporomandibular joint; CTS, cyclic tensile strain; iNOS, inducible NO synthase.

immune responses (3, 4). Targeted therapeutic strategies like neutralization of TNF- $\alpha$  or IL-1 activity by Abs or delivery of IL-1 receptor antagonist (IL-1Ra) reduces the severity of the disease in experimental and human RA (5). However, anti-inflammatory drugs are the choice treatment, whereas inhibitors of NF- $\kappa$ B or gene silencing of I $\kappa$ B kinase  $\beta$  (IKK $\beta$ ) are shown to suppress cartilage and bone erosion in experimental models of arthritis (6–9). To date most of these therapies have met with limited success, and arthritis remains one of the most common ailments and major causes of morbidity in the U.S. population.

Although the therapeutic potential of mobilization in restoring joint function in arthritic diseases is well recognized for centuries, relatively little is understood about the intracellular events underlying the actions of biomechanical signals in inflamed cartilage. These signals are essential for cartilage homeostasis, as evidenced by the findings that immobilization of healthy joints results in cartilage matrix loss (10). Chondrocytes embedded in the cartilage matrix constantly experience compressive, tensile, and shear forces during joint mobilization (11). These cells are mechanosensitive and can perceive and respond to biomechanical signals transduced by cell surface molecules such as  $\beta$  integrins and focal adhesion complexes (11–15). At high or traumatic magnitudes, biomechanical signals trigger expression of proinflammatory genes in chondrocytes, and at low physiological magnitudes, these signals are potent inhibitors of IL-1 $\beta$ - and TNF- $\alpha$ -dependent proinflammatory gene transcription (16–18). Furthermore, at low magnitudes these signals induce proteoglycan and collagen type II synthesis essential for cartilage homeostasis and repair (16–21).

TGF- $\beta$ -activating kinase, TAK1, is a critical regulator of the inducible transcription factor NF- $\kappa$ B, and thus plays a pivotal role in regulating downstream signaling events that mediate proinflammatory gene transcription. In Tak1<sup>m/m</sup> cells, signaling initiated by TNF/IL-1 and TLR-3 and -4 is severely impaired. However, cells lacking TAK1-associated binding proteins (TAB)-1 and -2 exhibit normal NF- $\kappa$ B activation. This indicates that TAK1, and not TAB-1/-2, is the critical point where signals generated by all three major proinflammatory molecules converge to activate NF- $\kappa$ B signaling cascade (22). TAK1 in turn activates the signalosome, a complex comprising three distinct I $\kappa$ B kinases (IKK), IKK $\alpha$ , IKK $\beta$ , and IKK $\gamma$ . In canonical pathway, upon phosphorylation by IKK $\beta$ , I $\kappa$ B $\alpha$  and I $\kappa$ B $\beta$ , the cytoplasmic inhibitors of NF- $\kappa$ B, are marked for ubiquitination and subsequent proteosomal degradation. The degradation of I $\kappa$ B $\alpha$  and I $\kappa$ B $\beta$  allows phosphorylation of NF- $\kappa$ B at multiple sites in a stimulant-dependent manner and its transmigration to the nucleus. The binding of NF- $\kappa$ B to its consensus sequences leads to transcription of a plethora of genes including proinflammatory cytokines and mediators, as well as several of the molecules required for the activation of NF- $\kappa$ B signaling cascade. Although this classical model of NF- $\kappa$ B activation by TNF- $\alpha$  or IL-1 $\beta$  is well documented, its complexity evolves from its regulation at multiple intracellular levels, in a cell as well as stimulus-dependent manner.

Because biomechanical signals inhibit proinflammatory gene transcription, we examined whether these signals regulate specific steps in the NF- $\kappa$ B pathway to attenuate the proinflammatory responses. Fibrochondrocytes (FCs) from the fibrocartilagenous disk of the temporomandibular joint (TMJ) were isolated by enzymatic digestion (23), and exposed to cyclic tensile strain (CTS) to mimic tensile forces perceived by cells during TMJ mobilization (17, 23). To investigate the mechanisms of anti-inflammatory actions of

biomechanical signals with in the NF- $\kappa$ B signaling cascade, cells were exposed to IL-1 $\beta$  as a proinflammatory signal, CTS alone, or simultaneously to CTS and IL-1 $\beta$ , and compared with control untreated cells. Following exposure to CTS and/or IL-1 $\beta$  for various time intervals, cells were harvested to examine the mRNA expression, regulation of proteins and their nuclear and cytoplasmic localization, within the NF- $\kappa$ B pathway.

## Materials and Methods

### Fibrochondrocyte harvesting and cell culture

Articular discs of the TMJs of 10- to 12-wk-old female ( $n = 6$ ) Sprague-Dawley rats (Harlan) were harvested and pooled to isolate FCs. All procedures were conducted following approval by the Institutional Laboratory Animal Care and Use Committee at The Ohio State University. Fibrocartilage pieces were minced in HBSS (Invitrogen), transferred onto a macroporous filter (Spectra/Mesh) and placed in a digestion chamber. After treatments for 10 min with 0.2% trypsin and 2 h with 0.2% collagenase type II (Worthington Biochemical), cells released from the cartilage were pelleted at  $800 \times g$  for 5 min, and washed twice with HBSS. The cells were then cultured in TCM (DMEM/F12, 1:1) (Mediatech), 10% FBS (HyClone), 10  $\mu$ g/ml penicillin and 100 U/ml streptomycin (Mediatech), and 2 mM L-glutamine (Invitrogen). Primary cultures of FCs were used during the first three passages. Between these passages cell morphology and the mRNA expression for phenotypic markers, aggrecan, biglycan, versican, and sox-9 were stable (20). All experiments were repeated with at least three different batches of primary cells prepared as described above using six rats each time.

### Application of CTS and proinflammatory agent

Cells ( $5 \times 10^4$ /well) were grown for 3–4 days on collagen I-coated BioFlex 6-well culture plates (Flexcell International) to 80% confluence in 5% CO<sub>2</sub> and 37°C. Twenty four hours before start of the experiments the medium was replaced with TCM containing 1% FBS. At the start of experiments, the plates were placed onto a Flexcell loading station and subjected to CTS at a magnitude of 12% and frequency of 0.05 Hz in the presence or absence of the stimulant IL-1 $\beta$ , TNF- $\alpha$ , or LPS. Four different treatment regimens were assigned: 1) untreated controls, 2) cells treated with recombinant human IL-1 $\beta$  (1 ng/ml; rhIL-1 $\beta$ ; Calbiochem), 3) cells treated with CTS, 4) cells treated with CTS and rhIL-1 $\beta$  concomitantly. The concentration of each stimulating agent was predetermined by titrating the iNOS mRNA induction in FCs and used at the optimal concentrations of 2 ng/ml IL-1 $\beta$ , 5 ng/ml TNF- $\alpha$ , and 10  $\mu$ g/ml LPS. The FCs were activated for 3 h where mRNA expression for NOS2A and MMP-13 was in the linear phase.

### Analysis of mRNAs expression by real-time PCR

RNA was isolated using the RNeasy Mini kit as recommended by the manufacturer (Qiagen). RNA (1  $\mu$ g) was reverse transcribed into cDNA in a total volume of 30  $\mu$ l using 200 units of Moloney murine leukemia virus, first at 42°C for 25 min and then at 65°C for 5 min. Real-time PCR was performed in a volume of 25  $\mu$ l on a Bio-Rad iCycler iQ (Bio-Rad) as described previously (24). Following primers and probes were used: iNOS-sense 5'-TTCTGTGCTAATGCGGAAGGT-3', iNOS-anti-sense 5'-

GCTTCCGACTTTCTGTCTCA-3', iNOS-probe 5'-CCGCGTCAGAGCCACAGTCCT-3'; IκBα-sense 5'-GGTATACTTAGCACCACAGCACACA-3', I-κBα-anti-sense 5'-CCCCAAATTTACAAGAACAACA-3', IκBα-α-probe 5'-CCTAGCCCCGAGCATTCTATTGTGGTGAT-3'; IκBβ-sense 5'-CCATGTAGCTGTCATCCACAAAG-3', IκBβ-anti-sense 5'-ACGTAGGCTCCGGTTTATGAG-3', IκBβ-probe 5'-AGAGATGGTCCAAGTCTCAGGGATGCT-3', MMP-13-sense 5'-GTTCAAGGAATCCAGTCTCTCTATGG-3'; MMP-13-anti-sense 5'-TGGGTACACTTCTCTGGTGTTT-3'; MMP-13-probe 5'-CCAGGAGAAGACCCCAACCCTAAGC-3'. Reactions were performed as follows: cycle I (1×): 95°C for 3.0 min, cycle II (50×): step 1 at 95°C for 0.3 min, followed by step 2 at 55°C for 0.3 min, and step 3 at 72°C for 30 min, cycle III at 40°C hold. Following amplification, a melting curve was obtained to ensure that primerdimers or nonspecific products had been eliminated or minimized. The data, obtained by real-time PCR, were analyzed by the comparative threshold cycle (CT) method. In this method, the amount of the target, normalized to GAPDH, and relative to a calibrator (either untreated sample or IL-1β-stimulated cells), is given by  $2^{-CT}$ , where  $CT = CT(\text{sample}) - CT(\text{calibrator})$ , and CT is the CT of the target gene subtracted from the CT of GAPDH.

### Protein phosphorylation and degradation

Activation and synthesis of transcription factors was analyzed by Western blot analysis. Total cell extracts (20 μg/lane) were separated by SDS-10% PAGE (SDS-PAGE) and blotted on polyvinylidene difluoride membranes (Bio-Rad). The blots were probed with anti-IκBα, anti-IκBβ (Santa Cruz Biotechnology), and phospho-IκBα Ser32, and Ser36, phospho-NF-κB p65 Ser536, and Ser276, anti-NF-κB p65, anti-TAK1 and phospho-TAK1 Thr187 (Cell Signaling) Abs and the binding of primary Abs revealed with IRDye-conjugated secondary Abs (LI-COR Biosciences). The blots were imaged with the Odyssey Infrared Imaging System and software (LI-COR Biosciences) at 700 and 800 nm channels and 169 μm resolution. Each band in all gels was analyzed in triplicate.

### Estimation of IKK-α activation

IKK activation in response to IL-1β and CTS was investigated as was described earlier (25). In brief, cells were suspended in lysis buffer (LB; 20 mM Tris (pH 8.0), 0.5 M NaCl, 0.25% Triton X-100, 1 mM EDTA, 1 mM EGTA, 10 mM β-glycerolphosphate), for 20 min at 4°C. IKK complexes were immunoprecipitated with anti-IKK-γ Abs (Santa Cruz Biotechnology) from a total of 250 μg of protein, washed with LB and then incubated with 2 μg of GST-IκBα conjugated to agarose beads (Santa Cruz Biotechnology) and 0.5 μmol of cold ATP at 30°C for 2 h. The beads were thoroughly washed with kinase buffer and the GST-IκBα was size separated by SDS-10% PAGE, transferred to nitrocellulose membranes and probed with either anti-phospho-Ser23/25-IκBα (Cell Signaling) or anti-GST Abs (Pharmacia). IRDye 800 goat anti-rabbit Ab or IRDye 680 goat anti-mouse Ab was used as a second Ab. The blots were imaged in triplicates with the Odyssey Infrared imaging system and software (LI-COR Biosciences) at 700 and 800 nm channels and 169 μm resolution.

## Immunofluorescence

Activation and synthesis of NF- $\kappa$ B, I $\kappa$ B $\alpha$ , and I $\kappa$ B $\beta$  was assessed by immunofluorescence using rabbit anti-NF- $\kappa$ B p65 IgG, anti-I $\kappa$ B- $\alpha$ , anti-I $\kappa$ B- $\beta$  or mouse anti-I $\kappa$ B $\alpha$  mAbs for double staining (Santa Cruz Biotechnology) as primary Abs and Cy2- or Cy3-conjugated goat anti-rabbit IgG as secondary Ab (The Jackson Laboratory). The stained cells on Bioflex membranes were mounted and visualized under a Zeiss Axioimage epifluorescence microscope and densitometrically analyzed using Zeiss Axiovision software (Zeiss).

## EMSA

Native polyacrylamide gels (5%) were prepared in Tris-borate-EDTA buffer. Fifty nanomoles of IRDye-labeled NF- $\kappa$ B consensus oligonucleotides (5'-AGTTGAGGGGACTTTCCAGGC-3'; 3'-TCAACTCCCCTGAAAGGGTCCG-5' LI-COR Biosciences) were added to the EMSA binding buffer (Lightshift EMSA kit; Pierce). A total of 20  $\mu$ g of nuclear proteins from cells exposed to various treatment regimens were added to the mixture, and incubated at room temperature for 20 min. The protein-DNA complexes were separated from unbound DNA by electrophoresis through a 5% nondenaturing polyacrylamide gel at 100 V for 1 h in a 0.5  $\times$  TBE buffer. Subsequently the gel was transferred to and imaged on a LI-COR Odyssey infrared imaging system at 700 and 800 nm channels and 169  $\mu$ m resolution. The density of fluorescence in each band was measured in triplicate with the use of LI-COR imaging software.

## Immunoprecipitation of I $\kappa$ B $\alpha$ and NF- $\kappa$ B P65

Following treatment, FCs were treated with ice-cold RIPA buffer (50 mM Tris-HCl (pH 7.4) 150 mM NaCl, 0.1% SDS, 1% Nonidet P-40, 1% deoxycholic acid sodium) containing a mixture of protease inhibitors (Roche). A total of 150  $\mu$ g of protein from each sample of the precleared nuclear lysates was incubated with 2 mg of mouse anti-I $\kappa$ B $\alpha$  Ab, and 20 ml of protein A/G-Sepharose beads at 4°C overnight with end-over-end rotation. The precipitated immune complexes were separated on 10% SDS-PAGE, electrophoretically transferred to nitrocellulose membranes, probed with rabbit anti-NF- $\kappa$ B and rabbit anti-I $\kappa$ B $\alpha$  (diluted 1/1000) and the corresponding IRDye-conjugated secondary Abs, and visualized with LI-COR Odyssey infrared imaging system (LI-COR Biosciences). The densitometric analysis of the fluorescence in each band of NF- $\kappa$ B and I $\kappa$ B $\alpha$  estimated in triplicate with the use of LI-COR imaging software and represented as total NF- $\kappa$ B bound to I $\kappa$ B $\alpha$  in each sample.

## Statistical analysis

All data were analyzed by SPSS 13.0 software. At least three independent experiments were performed and the most representative data has been presented. Densitometric analysis of gels was conducted for semiquantitative analysis of the bands. One-way ANOVA and the post hoc multiple comparison Dunnett's test were used to for statistical analysis (\*,  $p < 0.05$ ) and comparisons were made between stretched IL-1 $\beta$ -treated cells and unstretched IL-1 $\beta$ -treated cells.

## Results

### CTS attenuates TNF- $\alpha$ , IL-1 $\beta$ , and LPS-induced NOS2A and MMP-13 induction

To explore the mechanisms of actions of biomechanical signals, we first investigated whether these signals inhibit proinflammatory gene induction by a variety of inflammatory mediators. In these experiments, FCs were exposed to CTS of predetermined low magnitudes (12% tension at 0.05 Hz) known to inhibit IL-1 $\beta$ -induced gene transcription (17, 23). Stimulation of FCs with three major proinflammatory mediators IL-1 $\beta$ , TNF- $\alpha$ , or LPS, individually or in combination, resulted in a significant increase in NOS2A and MMP-13 mRNA expression within 3 h. Consistent with the anti-inflammatory actions of biomechanical signals, CTS suppressed >50% of the iNOS and 70% of the MMP-13 mRNA expression induced by IL-1 $\beta$ , TNF- $\alpha$ , and LPS alone, and in combination with IL-1 $\beta$  and TNF- $\alpha$ , or IL-1 $\beta$ , TNF- $\alpha$ , and LPS (Fig. 1, *A* and *B*). NOS2A expression was not observed in untreated control cells or cells treated with CTS alone. This suggests that CTS at these magnitudes acts in an inflammatory signal-dependent manner to attenuate proinflammatory gene induction.

The above studies demonstrated that CTS suppressed proinflammatory gene induction induced by all the three inflammatory mediators, IL-1 $\beta$ , TNF- $\alpha$ , and LPS, requiring distinct receptors for cell activation. Therefore, we next examined whether CTS suppressed NOS2A induction by down-regulating receptors for TNF- $\alpha$ , IL-1 $\beta$ , and/or LPS. In these experiments, cells were pre-exposed to CTS for 1 h, before addition of IL-1 $\beta$ , TNF- $\alpha$ , or LPS, and the extent of NOS2A protein expression examined 15 h later. Cells were also exposed to IL-1 $\beta$ , TNF- $\alpha$ , or LPS in the presence or absence of CTS. In response to all three stimuli, FCs produced significantly robust levels of NOS2 (Fig. 1 *C*). Cells pre-exposed to CTS for 1 h, before addition of IL-1 $\beta$ , TNF- $\alpha$ , or LPS demonstrated NOS2A production that was similar to cells that were not pre-exposed to CTS, indicating that pre-exposure of cells to CTS did not down-regulate their receptors to impair their ability to respond to IL-1 $\beta$ , TNF- $\alpha$ , or LPS. As expected, cells exposed to CTS for 1 h and then exposed simultaneously to CTS and IL-1 $\beta$ , TNF- $\alpha$  or LPS, exhibited attenuation of NOS2 gene expression further confirming that pre-exposure of cells to CTS does not compromise their ability to respond to IL-1 $\beta$ , TNF- $\alpha$ , or LPS or the ability of CTS to suppress IL-1 $\beta$ , TNF- $\alpha$ , or LPS-induced NOS2 expression (Fig. 1 *C*).

### CTS inhibits IL-1 $\beta$ , TNF- $\alpha$ , and LPS-dependent TAK1 phosphorylation

Above experiments suggested that CTS intercepts a common target molecule used by all three proinflammatory stimuli to inhibit activation of NF- $\kappa$ B transcriptional activity. Signals generated by IL-1 $\beta$ , TNF- $\alpha$ , or LPS receptors converge at TAK1 to trigger its rapid activation while TAB1 and TAB2 are dispensable for activation of NF- $\kappa$ B (22). Therefore, we examined the CTS-mediated regulation of TAK1 activation, but not TAB1 and TAB2. IL-1 $\beta$  induces a rapid and transient phosphorylation of TAK1 that can be observed within 10 min, and is dephosphorylated by 30 min. The CTS mediated inhibition of TAK1 phosphorylation was also rapid and could be observed within 10 min of CTS treatment in the presence of IL-1 $\beta$ . In fact, CTS inhibited IL-1 $\beta$ , TNF- $\alpha$ , and LPS-induced TAK1 phosphorylation by 73, 84, and 56%, respectively, within 10 min (Fig. 2*A*). However a

complete inhibition of IL-1 $\beta$ -induced TAK1 phosphorylation by CTS was not observed in any of the experiments.

### CTS inhibits IL-1 $\beta$ -dependent IKK activation

IKK $\beta$ , the principal kinase in the classical NF- $\kappa$ B pathway phosphorylates I $\kappa$ B proteins marking them for degradation. Because IKK $\alpha$  and - $\beta$  are tightly bound to NEMO(IKK $\gamma$ ), through their NEMO-binding domain, IKK complexes from cells subjected to IL-1 $\beta$  alone or IL-1 $\beta$  and CTS for 10, 30, 60, and 90 min, were immunoprecipitated with anti-IKK $\gamma$  Abs. Subsequently, phosphorylation of GST-I- $\kappa$ B $\alpha$  at Ser residues 32 and 36 was assessed as a marker of IKK activation. The incubation of IKK complexes with GST-I- $\kappa$ B $\alpha$  in the presence of ATP exhibited minimal IKK activation in control cells or cells exposed to CTS alone. Within 10 min of IL-1 $\beta$  treatment, IKK induced robust phosphorylation of GST-I- $\kappa$ B $\alpha$  which was sustained until 90 min. However, in cells concomitantly exposed to CTS and IL-1 $\beta$ , a marked suppression of IL-1 $\beta$ -induced IKK activation and thus inhibition of phosphorylation of GST-I- $\kappa$ B $\alpha$  was observed at all time points tested (Fig. 2*B*). These observations indicated that CTS represses IKK activity.

### CTS inhibits phosphorylation, degradation, and synthesis of I $\kappa$ B $\alpha$

Because IKK $\beta$  phosphorylates I $\kappa$ B $\alpha$  for its ubiquitination and eventual proteosomal degradation, we next confirmed whether CTS mediated inhibition of IKK activation leads to inhibition of I $\kappa$ B $\alpha$  phosphorylation and degradation. Cells subjected to IL-1 $\beta$  alone or CTS and IL-1 $\beta$  for 10, 30, 60, or 90 min, were lysed and the levels of phosphorylated I $\kappa$ B $\alpha$  at Ser residues 32 and 36, examined by Western blot analysis. IL-1 $\beta$  induced phosphorylation of I $\kappa$ B $\alpha$  at all the time points, flagging it for degradation. CTS, however, inhibited the IL-1 $\beta$ -dependent phosphorylation of I $\kappa$ B $\alpha$  by 62, 88, 95, and 95%, at 10, 30, 60, and 90 min, respectively (Fig. 2*B*). Subsequently, Western blot analysis revealed that the IL-1 $\beta$ -induced increase in phosphorylation of I $\kappa$ B $\alpha$  was followed by a rapid degradation of I $\kappa$ B $\alpha$  during the first 30 min (Fig. 2*B*). However, in spite of an increase in the phosphorylation of I $\kappa$ B $\alpha$  at 60 and 90 min, an increase in total I $\kappa$ B $\alpha$  levels was observed due to its active synthesis (Fig. 2, *B* and *D*) and continued degradation (Fig. 2, *B* and *D*). Contrarily, simultaneous exposure of cells to IL-1 $\beta$  and CTS, resulted in a marked suppression of IL-1 $\beta$  induced I $\kappa$ B $\alpha$  degradation during the initial 30 min; however, I $\kappa$ B $\alpha$  levels decreased in the cytoplasm during the ensuing 60 min (Fig. 2, *B-D*).

I $\kappa$ B $\alpha$  has a remarkable functional diversity in the regulation of NF- $\kappa$ B transcriptional activation. In addition to sequestering the NF- $\kappa$ B in the cytoplasm, I $\kappa$ B $\alpha$  shuttles NF- $\kappa$ B from the nuclear to cytoplasmic compartments of the cell, to terminate its transcriptional activity. Therefore, we next determined the relative presence of I $\kappa$ B $\alpha$  in the cytoplasmic and nuclear compartments of cells by immunofluorescence. FCs following exposure to IL-1 $\beta$  alone demonstrated a rapid degradation of cytoplasmic I $\kappa$ B $\alpha$  in IL-1 $\beta$  treated cells during initial 30 min and its subsequent reexpression and degradation continued during the next 60 min (Fig. 2, *C* and *D*). Contrarily, FCs subjected to CTS and IL-1 $\beta$ , demonstrated inhibition of IL-1 $\beta$ -dependent I $\kappa$ B $\alpha$  degradation in the cytoplasm by CTS during initial 30 min. Subsequently, a reduction in the total I $\kappa$ B $\alpha$  was observed in cells exposed to IL-1 $\beta$  as well as to CTS and IL-1 $\beta$  (Fig. 2, *C* and *D*). Analysis of immunofluorescence in FCs following

simultaneous application of CTS and IL-1 $\beta$ , reflected a rapid and significant up-regulation of intranuclear I $\kappa$ B $\alpha$  within 10 min, and its translocation to perinuclear area in the next 20 min, followed by its decrease in the nucleus and cytoplasm at later time points (Fig. 2, C and D). Western blot analysis of the cytoplasmic and nuclear I $\kappa$ B $\alpha$  fractions further confirmed that in IL-1 $\beta$  treated cells I $\kappa$ B $\alpha$  is rapidly degraded. Strikingly, exposure of cells to CTS results in a rapid translocation of I $\kappa$ B $\alpha$  to the nucleus within first 10 min (Fig. 2D).

Because I $\kappa$ B $\alpha$  has the  $\kappa$ B response elements in its promoter region, and its transcription is regulated by NF- $\kappa$ B, we speculated that the loss of I $\kappa$ B $\alpha$  at 60 and 90 min in above experiments was due to inhibition of its synthesis by CTS (26, 27). Examination of I $\kappa$ B $\alpha$  mRNA expression in response to IL-1 $\beta$  demonstrated a rapid increase of I $\kappa$ B $\alpha$  mRNA, as compared with untreated control FCs. More importantly, CTS suppressed IL-1 $\beta$ -dependent increase in I $\kappa$ B $\alpha$  mRNA expression by 78%, 71% and 70% at 30, 60, and 90 min, respectively (Fig. 2E). Above observations collectively indicate that CTS suppresses IL-1 $\beta$ -induced I $\kappa$ B $\alpha$  phosphorylation, degradation, as well as its synthesis.

### CTS inhibits IL-1 $\beta$ induced degradation of I $\kappa$ B $\beta$

IKK $\beta$  activation by IL-1 $\beta$  also leads to I $\kappa$ B $\beta$  phosphorylation for its ubiquitination and degradation (26–28). I $\kappa$ B $\beta$ , by sequestering NF- $\kappa$ B in the cytoplasm plays a small but significant role in the NF- $\kappa$ B canonical signaling cascade. Therefore, we investigated the consequences of the inhibition of IKK activation by CTS on the I $\kappa$ B $\beta$  proteolytic degradation. Western blot analysis of FCs subjected to IL-1 $\beta$ , revealed a slow but sustained degradation of the I $\kappa$ B $\beta$  during the entire 10 to 90 min (Fig. 3A). On the contrary, cells concomitantly exposed to IL-1 $\beta$  and CTS, demonstrated I $\kappa$ B $\beta$  to be at levels similar to untreated control FCs, suggesting that CTS abrogated IL-1 $\beta$ -induced I $\kappa$ B $\beta$  degradation at all the time points tested (Fig. 3A). Similarly, I $\kappa$ B $\beta$  levels remained unchanged in FCs exposed to CTS alone. Immunofluorescence analysis further confirmed that CTS suppressed IL-1 $\beta$ -induced intracellular degradation of I $\kappa$ B $\beta$  (Fig. 3B). Although I $\kappa$ B $\beta$  promoter regions exhibit a  $\kappa$ B consensus sequence, NF- $\kappa$ B fails to transcriptionally activate the I $\kappa$ B $\beta$  gene transcription (29). However, following degradation of cytosolic I $\kappa$ B $\beta$  in response to IL-1 $\beta$ , an increase in its transcriptional activity is observed (30, 31).

### CTS represses NF- $\kappa$ B p65 transactivation and nuclear translocation

To gain insight into the mechanisms of CTS mediated suppression of NF- $\kappa$ B signaling, we further examined effects of CTS on IL-1 $\beta$ -induced NF- $\kappa$ B transactivation. Upon activation by IL-1 $\beta$ , I $\kappa$ B kinases phosphorylate Ser536, whereas phosphorylation of p65 at Ser276 by PKA is induced by degradation of the I $\kappa$ B proteins (30, 32). This phosphorylation of NF- $\kappa$ B p65 is a prerequisite for its transactivation in the nucleus. Western blot analysis of FCs showed that IL-1 $\beta$  induced rapid and sustained phosphorylation of NF- $\kappa$ B p65 at Ser536 between 10 and 90 min (Fig. 4A). In FCs, IL-1 $\beta$ -induced phosphorylation of NF- $\kappa$ B p65 at Ser536 was inhibited by CTS at 30 and 90 min (Fig. 4A), whereas phosphorylation of Ser276 was not regulated by CTS.

We next determined whether CTS represses IL-1 $\beta$ -induced NF- $\kappa$ B p65 binding to the DNA. In these experiments, FCs subjected to IL-1 $\beta$ , or IL-1 $\beta$  and CTS for 10 to 90 min were lysed



and the nuclear proteins analyzed by EMSA. As shown in Fig. 4B, nuclear extracts from cells treated with IL-1 $\beta$  alone demonstrated progressively increased binding of NF- $\kappa$ B p65 to DNA, between 10 to 90 min. CTS markedly inhibited IL-1 $\beta$ -induced NF- $\kappa$ B p65 binding to its consensus sequences during the entire period examined. Further examination of the subunit structure of NF- $\kappa$ B regulated by CTS revealed that CTS abrogated binding of NF- $\kappa$ B heterodimers composed of p65 (Fig. 4B). However, DNA binding of other subunits of NF- $\kappa$ B, such as Rel B, c-rel, p105, or p52 was not found to bind DNA in response to IL-1 $\beta$  and/or CTS (data not shown).

### CTS regulates I $\kappa$ B $\alpha$ nuclear transport

Unphosphorylated form of I $\kappa$ B $\alpha$  enters the nucleus to bind NF- $\kappa$ B and its nuclear export signal allows transport of nuclear NF- $\kappa$ B-I $\kappa$ B $\alpha$  complexes back to the cytosol, thereby terminating its transcriptional activity (26, 30). In above studies we observed that following simultaneous exposure to CTS and IL-1 $\beta$ , 1) I $\kappa$ B $\alpha$  rapidly translocates to the nucleus within 10 min, and 2) NF- $\kappa$ B that translocates to the nucleus during initial 10 to 30 min, does not bind to its consensus sequences. To visualize the temporal regulation of I $\kappa$ B $\alpha$  and NF- $\kappa$ B in the cytoplasmic and nuclear compartments, FCs were activated as described above and the presence of NF- $\kappa$ B p65 and I $\kappa$ B $\alpha$  in the nuclear and cytoplasmic compartments examined in the same cells by immunofluorescence. Following exposure to IL-1 $\beta$  alone, a rapid degradation of cytoplasmic I $\kappa$ B $\alpha$  was paralleled by a rapid translocation of NF- $\kappa$ B to the nucleus (Fig. 4D). FCs subjected to CTS and IL-1 $\beta$  demonstrated that CTS inhibited IL-1 $\beta$ -dependent I $\kappa$ B $\alpha$  degradation, however, it induced a rapid up-regulation of intranuclear I $\kappa$ B $\alpha$  during the initial 10 min. Simultaneous visualization of NF- $\kappa$ B in these cells revealed retention of cytoplasmic NF- $\kappa$ B, even though translocation of NF- $\kappa$ B to a lesser extent in the nuclei was apparent during the initial 10 min (Fig. 4D). As observed above, examination of FCs after ensuing 20 min of IL-1 $\beta$  treatment, exhibited negligible presence of I $\kappa$ B $\alpha$  in the nuclei or cytoplasm, and in parallel nuclear translocation of nearly all NF- $\kappa$ B. Contrarily in FCs treated with CTS and IL-1 $\beta$ , majority of the I $\kappa$ B $\alpha$  and NF- $\kappa$ B were present in the perinuclear area and cytoplasm, with presence of remaining I $\kappa$ B $\alpha$  and NF- $\kappa$ B in the nuclei. Interestingly, following 60 and 90 min of activation of FCs with IL-1 $\beta$ , the levels of I $\kappa$ B $\alpha$  and NF- $\kappa$ B progressively increased in the nucleus and in the cytoplasm. Noticeably, in FCs exposed to IL-1 $\beta$  and CTS simultaneously, the I $\kappa$ B $\alpha$  levels were lower in the cytoplasm, with a clear lack of intranuclear I $\kappa$ B $\alpha$  and NF- $\kappa$ B by 90 min. These observations further demonstrated that CTS up-regulates I $\kappa$ B $\alpha$  nuclear trafficking to facilitate NF- $\kappa$ B export from the nucleus to terminate NF- $\kappa$ B transcriptional activity.

To further confirm the relevance of I $\kappa$ B $\alpha$  nuclear translocation in NF- $\kappa$ B signaling, the nuclear extracts from FCs subjected to IL-1 $\beta$  in the presence or absence of CTS were subjected to coimmunoprecipitation with anti-I $\kappa$ B $\alpha$  and anti-NF- $\kappa$ B p65 immunoglobulins, and analyzed by Western blots. The presence of NF- $\kappa$ B or I $\kappa$ B $\alpha$  was negligible in untreated control cells as well as cells exposed to CTS alone. FCs treated with IL-1 $\beta$  exhibited presence of nuclear NF- $\kappa$ B and I $\kappa$ B $\alpha$  but insignificant NF- $\kappa$ B-I $\kappa$ B $\alpha$  complexing during the first 30 min of activation, and their subsequent up-regulation in nuclear compartment at 60 and 90 min. More importantly, simultaneous exposure of CTS and IL-1 $\beta$  demonstrated a dramatic up-regulation of NF- $\kappa$ B-I $\kappa$ B $\alpha$  complexes in nuclei during first 30 min and their

subsequent decrease in the ensuing 60 min (Fig. 4C). Collectively, these findings strongly demonstrate that CTS, in addition to inhibiting TAK1 activity, induces a rapid I $\kappa$ B $\alpha$  nuclear translocation to facilitate quick export of nuclear NF- $\kappa$ B to prevent its transcriptional activity and subsequent proinflammatory gene induction (Fig. 5).

## Discussion

Our observations demonstrate that tensile forces of low/physiologic levels attenuate inflammatory gene induction by three major proinflammatory molecules, IL-1 $\beta$ , TNF- $\alpha$ , and LPS, individually and collectively, by inhibiting a critical event in the NF- $\kappa$ B activation. All of these mediators act on cells via discrete receptors to initiate inflammatory responses (30, 31, 33). Signals generated by CTS do not down-regulate receptors for IL-1 $\beta$ , TNF- $\alpha$ , or LPS as a mechanism to inhibit proinflammatory signaling cascade. The fact that IL-1 $\beta$ , TNF- $\alpha$  and LPS all stimulated the production of NOS2A in cells preexposed to CTS for one hour to an extent observed in control FCs without exposure to CTS, suggests that CTS does not down-regulate cell surface receptors but may intercept specific intracellular events in the NF- $\kappa$ B signaling cascade.

Signals generated by the binding of major inflammatory ligands to their specific receptors converge at TAK1 via activation of discrete intermediate mediators and co-adaptors. CTS inhibits IL-1 $\beta$ , TNF- $\alpha$ , or LPS induced phosphorylation of TAK1 at Thr187 necessary for its kinase activity. The reduction in TAK1 activation substantially decreased IL-1 $\beta$ -dependent induction of IKK activity and phosphorylation of I $\kappa$ B $\alpha$  at Ser residues 32 and 36 by the IKK complexes. This provides evidence that CTS regulates TAK1, a critical control point in the NF- $\kappa$ B signaling cascade, to limit transcriptional activity of NF- $\kappa$ B and resulting proinflammatory gene induction. Inactivation of IL-1 $\beta$ -induced TAK1 phosphorylation by CTS may be strategically a very important point to merge suppression of transcriptional activation of NF- $\kappa$ B by diverse proinflammatory signals before they activate the signalosome assembly. At this time it is not clear how CTS-induced signals check TAK1 phosphorylation induced by diverse receptors of IL-1 $\alpha$ , TNF- $\alpha$  and LPS. Mechanical signals are perceived by cells through  $\alpha_1/\beta_5$  integrin receptors on chondrocytes (34). How these signals then regulate TAK1 activity is as yet not clear.

Inhibition of IKK activity prevents I $\kappa$ B $\alpha$  and I $\kappa$ B $\beta$  phosphorylation and degradation, thus prolonging I $\kappa$ B $\alpha$  and I $\kappa$ B $\beta$  mediated cytoplasmic sequestration of NF- $\kappa$ B. CTS also down-regulates I $\kappa$ B $\alpha$  gene transcription, further repressing activation of NF- $\kappa$ B. Nevertheless, CTS was found not to completely block the synthesis of I $\kappa$ B $\alpha$  or I $\kappa$ B $\beta$  beyond levels of constitutive synthesis. Thus a pool of I $\kappa$ B $\alpha$  and I $\kappa$ B $\beta$  was always present in the cells, that contributed to sequestration of the NF- $\kappa$ B in the cytoplasm of cells after 60 min of CTS exposure.

Another way in which NF- $\kappa$ B activity could be potentially inhibited is by shuttling of NF- $\kappa$ B from the nucleus to terminate its transcriptional activity (30, 31, 33). In addition to inhibiting nuclear translocation of P65, CTS also abrogates DNA binding of P65 that rapidly translocates to the nucleus at the earlier time points. A nuclear export signal on I $\kappa$ B $\alpha$  allows shuttling of nuclear NF- $\kappa$ B to the cytoplasm, thereby providing yet another point of control

over NF- $\kappa$ B transcriptional activity (26, 30). CTS regulates shuttling of I $\kappa$ B $\alpha$  to further terminate NF- $\kappa$ B activity. During first 30 min of IL-1 $\beta$  treatment I- $\kappa$ B $\alpha$  is rapidly degraded and minimal nuclear import of I $\kappa$ B $\alpha$  is observed. Strikingly, CTS up-regulates rapid nuclear import of I $\kappa$ B $\alpha$  and its binding to NF- $\kappa$ B p65 within the first ten minutes, to export any NF- $\kappa$ B dimers that enter the nucleus. This binding of I $\kappa$ B $\alpha$  to NF- $\kappa$ B may also be responsible for preventing the binding of NF- $\kappa$ B to DNA observed in EMSA analysis. By 60 min the nuclear migration of I $\kappa$ B $\alpha$  was reduced, likely due to inhibition of IL-1 $\beta$  induced I $\kappa$ B $\alpha$  synthesis. However, the observed lack of NF- $\kappa$ B binding to the DNA by 60 min can be attributed to the suppression of NF- $\kappa$ B nuclear translocation by CTS. Thus, CTS suppresses IL-1-induced transcriptional activation of NF- $\kappa$ B at multiple levels by inhibiting TAK1 activation, suppressing I $\kappa$ B $\alpha$  degradation, inhibition of I $\kappa$ B $\alpha$  gene transcription, and promoting its nuclear shuttling to terminate NF- $\kappa$ B DNA binding.

TMJ is a compound articulation where the disc is exposed to notable compressive, tensile and shear forces. During joint movement, the disc elongates in antero-posterior axis, and experiences tensile forces around 8% on the balancing side and 16% on the working side (34). We have observed that FCs when exposed to tensile forces at a magnitude of 12% elongation inhibit proinflammatory responses. Although it is difficult to calculate the extent of forces exerted on the FCs during TMJ movement, the magnitude of forces used in our studies appear to be within the physiological range.

Fibrochondrocytes within the cartilage take an active role in cartilage degradation and repair by perceiving proinflammatory signals via discrete receptors as well as by perceiving mechanical signals to regulate proinflammatory responses (17–21). Chondrocytes and FCs both respond to mechanical signals in a magnitude-dependent manner. The anti-inflammatory actions of mechanical signals are observed at magnitudes close to those experienced by chondrocytes during normal joint movement (16, 17, 19, 20, 34). In this report we have shown for the first time, that at low magnitudes mechanical signals down-regulate activation of TAK1, to intercept intracellular proinflammatory responses generated by several different proinflammatory insults. Inhibition of TAK1 activation converges all proinflammatory signals into a central pathway to terminate NF- $\kappa$ B transcriptional activity. By inhibiting TAK1 activation these signals are potent suppressors of inflammation induced by diverse insults to the cells (Fig. 5). Inflammatory disorders of the joints are conventionally treated with various inhibitors of proinflammatory mediators. Recent efforts have sought to block critical steps in NF- $\kappa$ B signaling cascade to alleviate arthritic pain and cartilage destruction. However, mostly these measures have shown limited success and are shown to be accompanied by undesirable side effects. Mechanical signals at low physiological levels appear to generate an effective nonpharmacological signal that acts as a molecular switch of NF- $\kappa$ B activity to inhibit inflammation in fibrochondrocytes. This report provides the mechanisms underlying the well recognized but little understood role of mechanical signals in ameliorating inflammation of the joints.

## Acknowledgments

This work was supported by the National Institutes of Health by Grants AR04878, DE15399, AT00646, and HD40939.

## References

1. Gaffo A, Saag KG, Curtis JR. Treatment of rheumatoid arthritis. *Am. J. Health Syst. Pharm.* 2006; 63:2451–2465. [PubMed: 17158693]
2. Abramson SB, Yazici Y. Biologics in development for rheumatoid arthritis: relevance to osteoarthritis. *Adv. Drug Deliv. Rev.* 2006; 58:212–225. [PubMed: 16567019]
3. Sivalingam SP, Thumboo J, Vasoo S, Thio ST, Tse C, Fong KY. In vivo pro- and anti-inflammatory cytokines in normal and patients with rheumatoid arthritis. *Ann. Acad. Med. Singapore.* 2007; 36:96–94. [PubMed: 17364074]
4. Weissmann G. The pathogenesis of rheumatoid arthritis. *Bull. Hosp. J. Dis.* 2006; 64:12–15.
5. Moreland LW. Biologic therapies on the horizon for rheumatoid arthritis. *J. Clin. Rheumatol.* 2004; 10:S32–S39. [PubMed: 17043499]
6. Schopf L, Savinainen A, Anderson K, Kujawa J, DuPont M, Silva M, Siebert E, Chandra S, Morgan J, Gangurde P. IKK $\beta$  inhibition protects against bone and cartilage destruction in a rat model of rheumatoid arthritis. *Arthritis Rheum.* 2006; 54:3163–3173. [PubMed: 17009244]
7. Tas SW, Adriaansen J, Hajji N, Bakker AC, Firestein GS, Vervoordeldonk MJ, Tak PP. Amelioration of arthritis by intraarticular dominant negative Ikk  $\beta$  gene therapy using adeno-associated virus type 5. *Hum. Gene Ther.* 2006; 17:821–832. [PubMed: 16942442]
8. Clohisy JC, Roy BC, Biondo C, Frazier E, Willis D, Teitelbaum SL, Abu-Amer Y. Direct inhibition of NF- $\kappa$ B blocks bone erosion associated with inflammatory arthritis. *J. Immunol.* 2003; 171:5547–5553. [PubMed: 14607962]
9. Lianxu C, Hongti J, Changlong Y. NF- $\kappa$ Bp65-specific siRNA inhibits expression of genes of COX-2: NOS-2 and MMP-9 in rat IL-1 $\beta$ -induced and TNF- $\alpha$ -induced chondrocytes. *Osteoarthritis Cartilage.* 2006; 14:367–376. [PubMed: 16376111]
10. Ferretti M, Gassner R, Wang Z, Perera P, Deschner J, Sowa G, Salter RB, Agarwal S. Biomechanical signals suppress proinflammatory responses in cartilage: early events in experimental antigen-induced arthritis. *J. Immunol.* 2006; 177:8757–8766. [PubMed: 17142778]
11. Ateshian GA. Artificial cartilage: weaving in three dimensions. *Nat. Materials.* 2007; 6:89–90. [PubMed: 17268489]
12. Garcia AJ, Boettiger D. Integrin-fibronectin interactions at the cell-material interface: initial integrin binding and signaling. *Biomaterials.* 1999; 20:2427–2433. [PubMed: 10614947]
13. Goldmann WH. Mechanical aspects of cell shape regulation and signaling. *Cell Biol. Int.* 2002; 26:313–317. [PubMed: 11991660]
14. Hsieh MH, Nguyen HT. Molecular mechanism of apoptosis induced by mechanical forces. *Int. Rev. Cytol.* 2005; 245:45–90. [PubMed: 16125545]
15. Ingber DE. Tensegrity: the architectural basis of cellular mechanotransduction. *Annu. Rev. Physiol.* 1997; 59:575–599. [PubMed: 9074778]
16. Agarwal S, Deschner J, Long P, Verma A, Hofman C, Evans CH, Piesco N. Role of NF- $\kappa$ B transcription factors in antiinflammatory and proinflammatory actions of mechanical signals. *Arthritis Rheum.* 2004; 50:3541–3548. [PubMed: 15529376]
17. Agarwal S, Long P, Gassner R, Piesco NP, Buckley MJ. Cyclic tensile strain suppresses catabolic effects of interleukin-1 $\beta$  in fibrochondrocytes from the temporomandibular joint. *Arthritis Rheum.* 2001; 44:608–617. [PubMed: 11263775]
18. Ferretti M, Srinivasan A, Deschner J, Gassner R, Baliko F, Piesco N, Salter R, Agarwal S. Anti-inflammatory effects of continuous passive motion on meniscal fibrocartilage. *J. Orthop. Res.* 2005; 23:1165–1171. [PubMed: 16140197]
19. Gassner RJ, Buckley MJ, Studer RK, Evans CH, Agarwal S. Interaction of strain and interleukin-1 in articular cartilage: effects on proteoglycan synthesis in chondrocytes. *Int. J. Oral Maxillofac. Surg.* 2000; 29:389–394. [PubMed: 11071247]
20. Xu Z, Buckley MJ, Evans CH, Agarwal S. Cyclic tensile strain acts as an antagonist of IL-1  $\beta$  actions in chondrocytes. *J. Immunol.* 2000; 165:453–460. [PubMed: 10861084]
21. Deschner J, Hofman CR, Piesco NP, Agarwal S. Signal transduction by mechanical strain in chondrocytes. *Curr. Opin. Clin. Nutr. Metab. Care.* 2003; 6:289–293. [PubMed: 12690261]

22. Shim JH, Xiao C, Paschal AE, Bailey ST, Rao P, Hayden MS, Lee KY, Bussey C, Steckel M, Tanaka N, et al. TAK1, but not TAB1 or TAB2, plays an essential role in multiple signaling pathways in vivo. *Genes Dev.* 2005; 19:2668–2681. [PubMed: 16260493]
23. Deschner J, Rath-Deschner B, Agarwal S. Regulation of matrix metalloproteinase expression by dynamic tensile strain in rat fibrochondrocytes. *Osteoarthritis Cartilage.* 2006; 14:264–272. [PubMed: 16290189]
24. Deschner J, Wypasek E, Ferretti M, Rath B, Anghelina M, Agarwal S. Regulation of RANKL by biomechanical loading in fibrochondrocytes of meniscus. *J. Biomech.* 2006; 39:1796–1803. [PubMed: 16038916]
25. DiDonato JA. Assaying for I $\kappa$ B kinase activity. *Methods Enzymol.* 2000; 322:393–400. [PubMed: 10914035]
26. Hoffmann A, Levchenko A, Scott ML, Baltimore D. The I $\kappa$ B-NF- $\kappa$ B signaling module: temporal control and selective gene activation. *Science.* 2002; 298:1241–1245. [PubMed: 12424381]
27. Hayden MS, Ghosh S. Signaling to NF- $\kappa$ B. *Genes Dev.* 2004; 18:2195–2224. [PubMed: 15371334]
28. Senftleben U, Karin M. The IKK/NF- $\kappa$ B pathway. *Crit. Care Med.* 2002; 30:S18–S26.
29. Griffin BD, Moynagh PN. Persistent interleukin-1 $\beta$  signaling causes long term activation of NF $\kappa$ B in a promoter-specific manner in human glial cells. *J. Biol. Chem.* 2006; 281:10316–10326. [PubMed: 16455661]
30. Hayden MS, Ghosh S. Signaling to NF- $\kappa$ B. *Genes Dev.* 2004; 18:2195–2224. [PubMed: 15371334]
31. Moynagh PN. The NF- $\kappa$ B pathway. *J. Cell. Sci.* 2005; 118:4589–4592. [PubMed: 16219681]
32. Buss H, Dorrie A, Schmitz ML, Frank R, Livingstone M, Resch K, Kracht M. Phosphorylation of serine 468 by GSK-3 $\beta$  negatively regulates basal p65 NF- $\kappa$ B activity. *J. Biol. Chem.* 2004; 279:49571–49574. [PubMed: 15465828]
33. Pomerantz JL, Baltimore D. Two pathways to NF- $\kappa$ B. *Mol. Cell.* 2002; 10:693–695. [PubMed: 12419209]
34. Sindelar BJ, Herring SW. Soft tissue mechanics of the temporomandibular joint. *Cells Tissues Organs.* 2005; 180:36–43. [PubMed: 16088132]

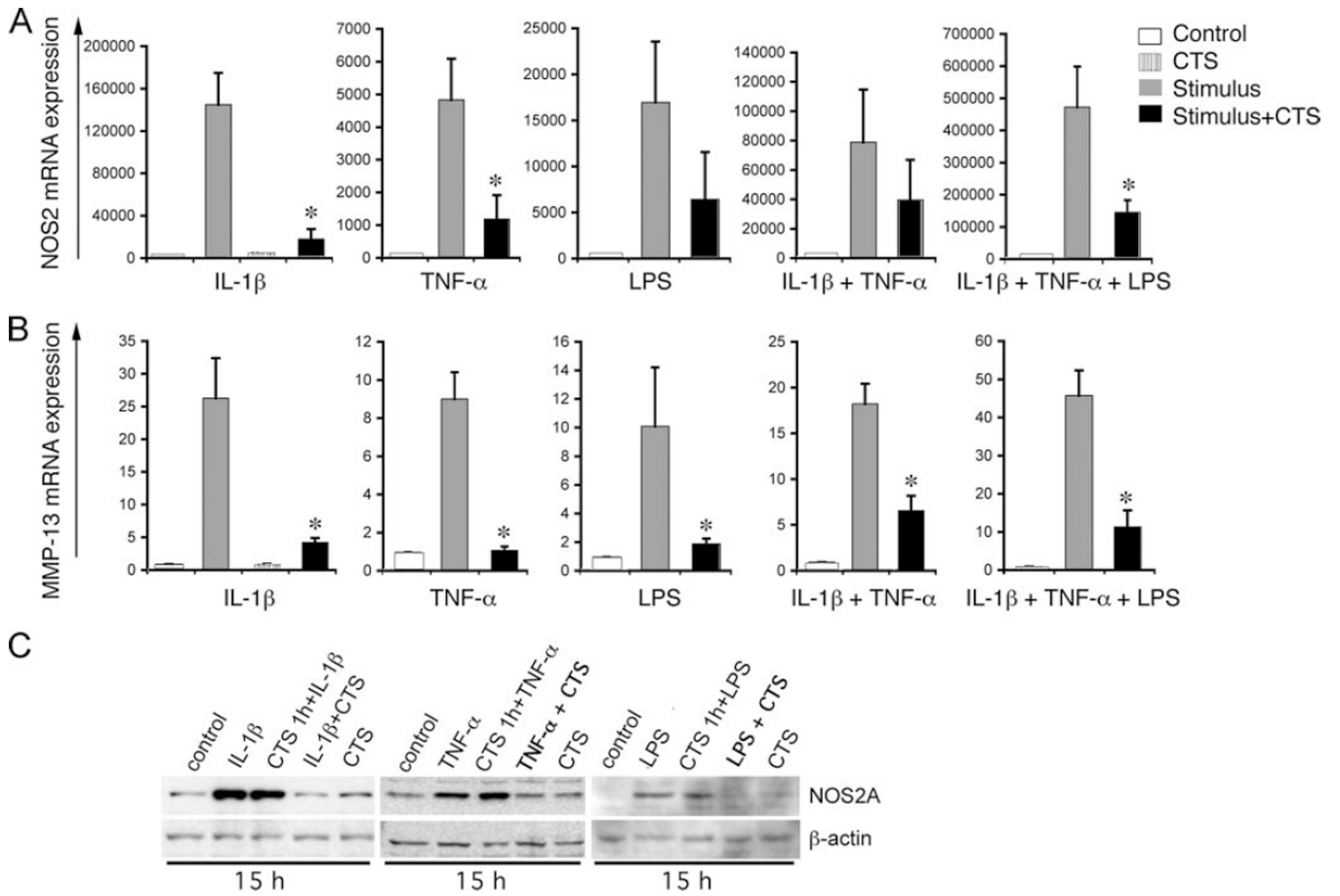


**FIGURE 1.**

CTS inhibits IL-1β, TNF-α, and LPS-induced NOS2A (A) and MMP-13 (B) mRNA expression. FCs were treated with IL-1β (1 ng/ml); TNF-α (5 ng/ml); or LPS (10 μg/ml) individually or in combination in the absence or presence of the simultaneous exposure to CTS for 3 h, and mRNA expression assessed by real-time PCR. C, Expression of NOS2A protein in control untreated FCs, FCs exposed to stimulants (IL-1β, TNF-α, or LPS at above concentrations); FCs pre-exposed to CTS for 1 h before addition of stimulants, FCs exposed simultaneously to stimulant and CTS, or FCs exposed to CTS alone for 15 h. Western blots exhibit induction of NOS2A in cells exposed to stimulant with or without pre-exposure to CTS, whereas inhibition of NOS2A expression in cells exposed simultaneously to stimulants and CTS. \*,  $p < 0.5$ .

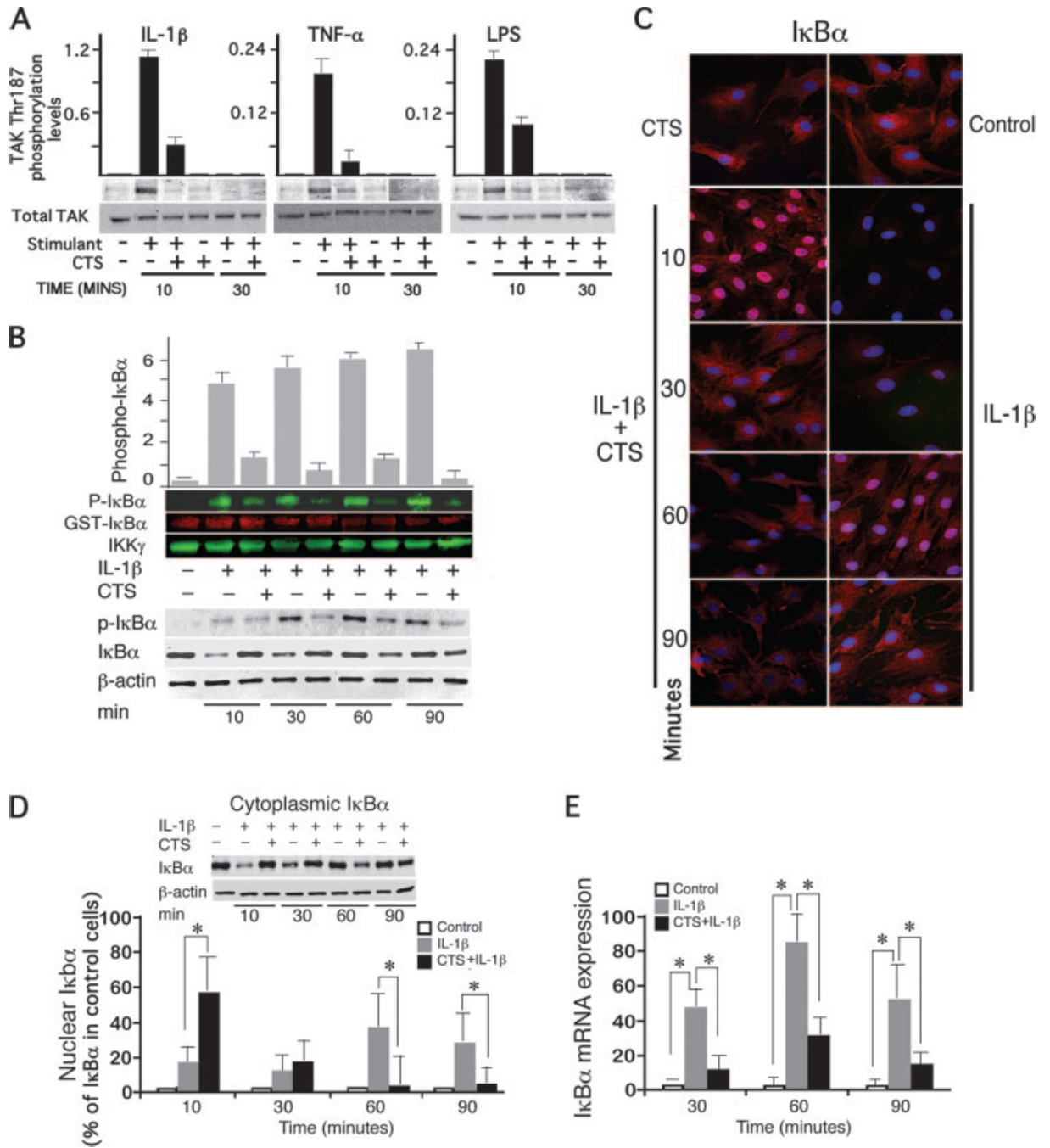


**FIGURE 2.**

CTS suppresses IL-1 $\beta$ -induced TAK1 activation and I $\kappa$ B $\alpha$  activation. *A*, Phospho-TAK1 (Thr187)/total TAK1 in IL-1 $\beta$ , TNF- $\alpha$ , or LPS-activated FCs and inhibition of phosphorylation by CTS during the initial 10 and 30 min of activation. *B*, Phosphorylation of GST-I $\kappa$ B $\alpha$  by IKK complexes immunoprecipitated with anti-IKK $\gamma$  Abs from lysates of cells exposed to IL-1 $\beta$  in the presence or absence of CTS for 10 to 90 min. Western blots were probed with anti-phospho-I $\kappa$ B $\alpha$  mouse mAb (*p*-I $\kappa$ B $\alpha$ ), and anti-N-terminal-I $\kappa$ B-GST IgG as I $\kappa$ B loading control. The total IKK levels were assessed by probing the blots with

rabbit anti-IKK $\gamma$  IgG. The densitometric imaging with infra-red IRdye 680 or 800 labeled secondary Abs shows that CTS inhibited IL-1 $\beta$ -induced activation of IKK. In same cells, Western blot analysis showed that CTS inhibited IL-1 $\beta$ -induced phosphorylation of I $\kappa$ B $\alpha$  at Ser32 and Ser36, degradation and synthesis. *C*, Immunofluorescence analysis with anti-I $\kappa$ B $\alpha$  Abs showing that CTS inhibits IL-1 $\beta$ -dependent degradation and synthesis of I $\kappa$ B $\alpha$ . The nucleus has been stained with DAPI and I $\kappa$ B $\alpha$  has been shown in red using CY3. Pink areas in the nucleus indicate increased presence of I $\kappa$ B $\alpha$ . *D*, Western blot analysis of cytoplasmic and nuclear I $\kappa$ B $\alpha$  levels in FCs of I $\kappa$ B $\alpha$  showing a CTS-induced influx of I $\kappa$ B $\alpha$  into the nucleus within 10 min and inhibition of its degradation in the cytoplasm. *E*, I $\kappa$ B $\alpha$  mRNA expression in FCs exhibiting inhibition of IL-1-dependent I $\kappa$ B $\alpha$  mRNA expression by CTS. *A* and *B*, one of three separate experiments with similar results using different primary chondrocyte cultures. The bars in *A* and *B* represent mean and SEM of densitometric analysis of gels shown. Data in *C* represents one of three separate experiments with similar results. Data in *D* and *E* represents mean and SEM of three experiments performed in duplicates. Inset in *D* represents one of three separate experiments. \*,  $p < 0.05$ .



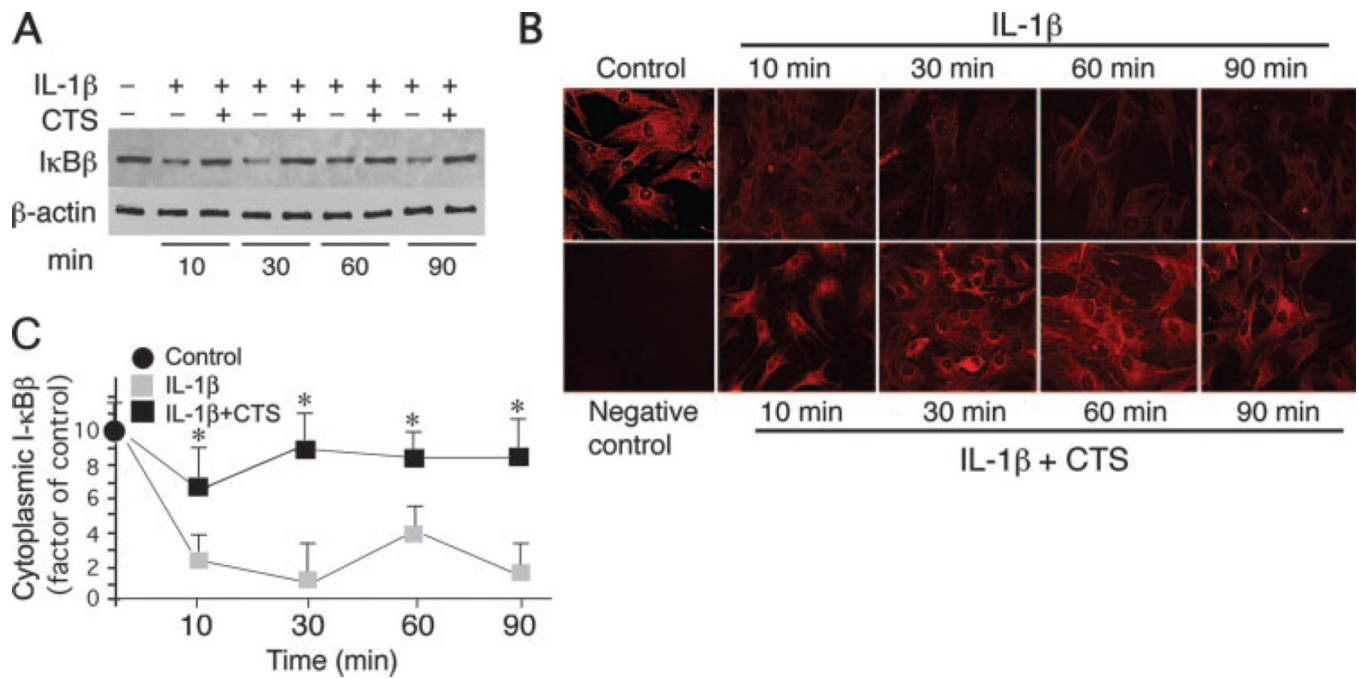


**FIGURE 3.** CTS inhibits IL-1β-induced I-κBβ degradation. *A*, Western blot analysis showing the inhibition of IL-1-induced IκBβ degradation by CTS. *B*, Immunofluorescence analysis demonstrating inhibition of IκBβ degradation by CTS. *C*, Densitometric analysis of IκBβ degradation in FCs exposed to IL-1β in the presence or absence of CTS. Data represents one of three separate experiments with similar results in *A* and *C*, and mean and SD of three separate experiments in *B*. \*,  $p < 0.05$ .

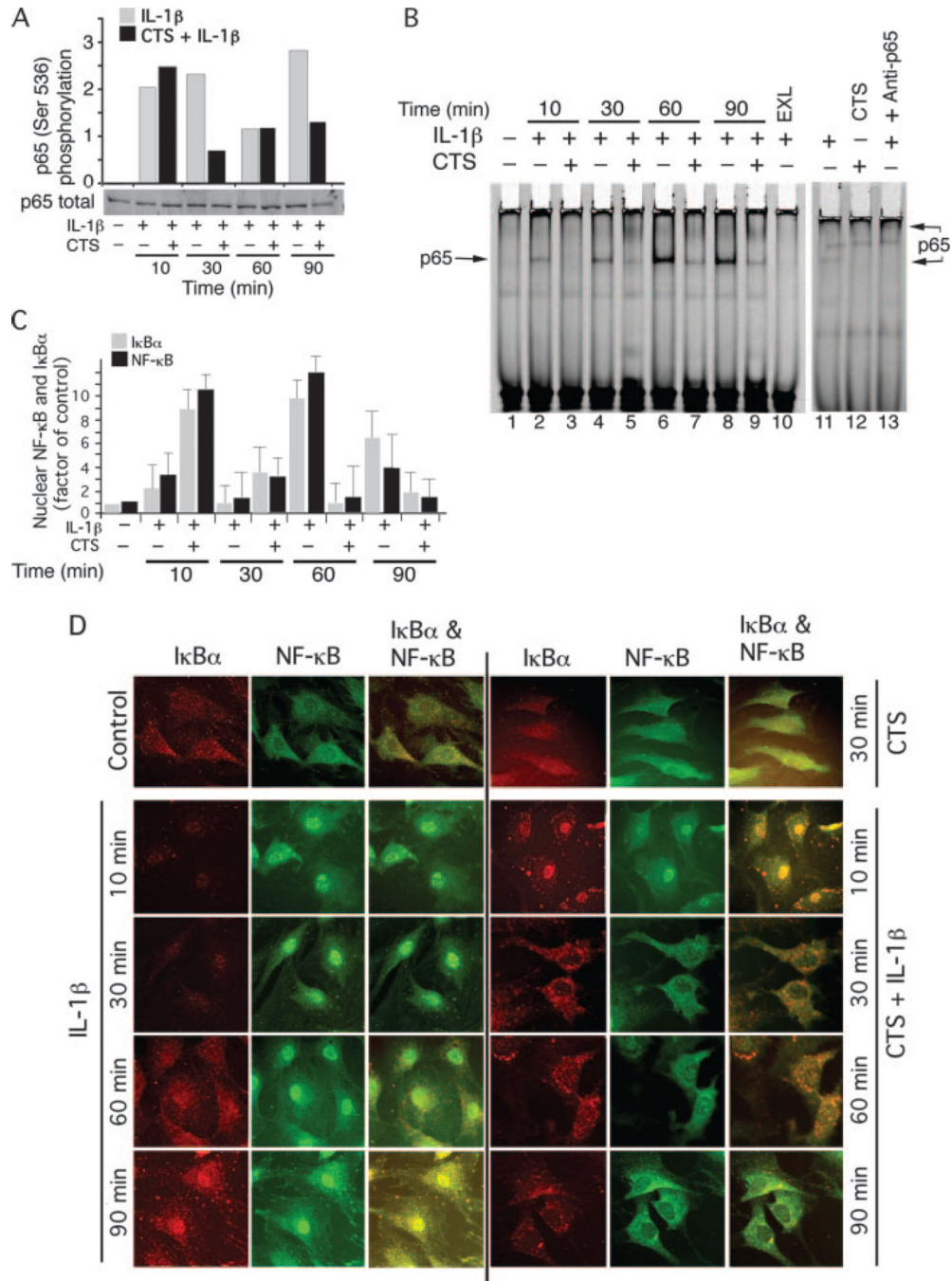


**FIGURE 4.** CTS inhibits IL-1β-induced NF-κB phosphorylation, nuclear translocation and DNA binding. *A*, Western blot analysis of FC lysates showing CTS inhibits IL-1β-induced phosphorylation of NF-κB p65 at Ser536 at 30 and 90 min as assessed by densitometric imaging of IRdye 680 labeled secondary Abs. *B*, EMSA analysis exhibiting DNA binding of NF-κB p65 from the 20 μg of nuclear extracts of FCs showing lack of DNA binding in untreated control FCs (*lane 1*); increased binding of NF-κB p65 in IL-1β-treated cells (*lanes 2, 4, 6, and 8*); and inhibition of NF-κB binding to DNA in cells treated with CTS and IL-1β

(lanes 3, 5, 7, and 9). IL-1 $\beta$  treated cells incubated with 100-fold excess unlabeled probe (lane 10), cells exposed to IL-1 $\beta$  and control IgG (lane 11), CTS alone (lane 12), and super shift EMSA showing CTS regulates NF- $\kappa$ B subunit p65 to DNA (lane 13). *C*, Complexing of I $\kappa$ B $\alpha$  with NF- $\kappa$ B p65 following treatment of FCs with IL-1 $\beta$  in the presence or absence of CTS was analyzed in the immunoprecipitates of I $\kappa$ B $\alpha$ . Western blot analysis showed the binding of NF- $\kappa$ B to I $\kappa$ B $\alpha$  in cells exposed to CTS and IL-1 $\beta$  and a lack of I $\kappa$ B $\alpha$ -NF- $\kappa$ B complexes during the initial 10 min of activation. However, at 60 min the presence of I $\kappa$ B $\alpha$ -NF- $\kappa$ B complexes was apparent in IL-1 $\beta$ -treated cells, whereas a lack of such complexes was observed in cells exposed to CTS and IL-1 $\beta$ . *D*, Immunostaining of NF- $\kappa$ B (green) and I $\kappa$ B $\alpha$  (red) and their merged images in FCs treated with IL-1 $\beta$  (*left panel*) or CTS and IL-1 $\beta$  (*right panel*) at 10, 30, 60, or 90 min. FCs exhibit that IL-1 $\beta$  induces rapid and sustained translocation of NF- $\kappa$ B to the nucleus. CTS induces rapid translocation of I $\kappa$ B $\alpha$  to the nucleus, and increases complexing with the minimal NF- $\kappa$ B that enters into the nucleus during first 10 min due to the rapid actions of IL-1 $\beta$ . This I $\kappa$ B $\alpha$  shuttles the nuclear NF- $\kappa$ B out, as evidenced by the presence of yellow stain in the nuclei and the presence of I $\kappa$ B $\alpha$ -NF- $\kappa$ B complexes in the cytoplasm. The I $\kappa$ B $\alpha$ -NF- $\kappa$ B complexes are also evident after 30 and 60 min in the cytoplasm of the cells treated with CTS and IL-1 $\beta$ , suggesting nuclear export of NF- $\kappa$ B by I $\kappa$ B $\alpha$ . This confirms the findings from *B* and *C*. The data in *A*, *B*, and *D* is representative of one of three separate experiments using three separate primary cell cultures. The data in *C* shows mean and SEM of gels in two separate experiments.

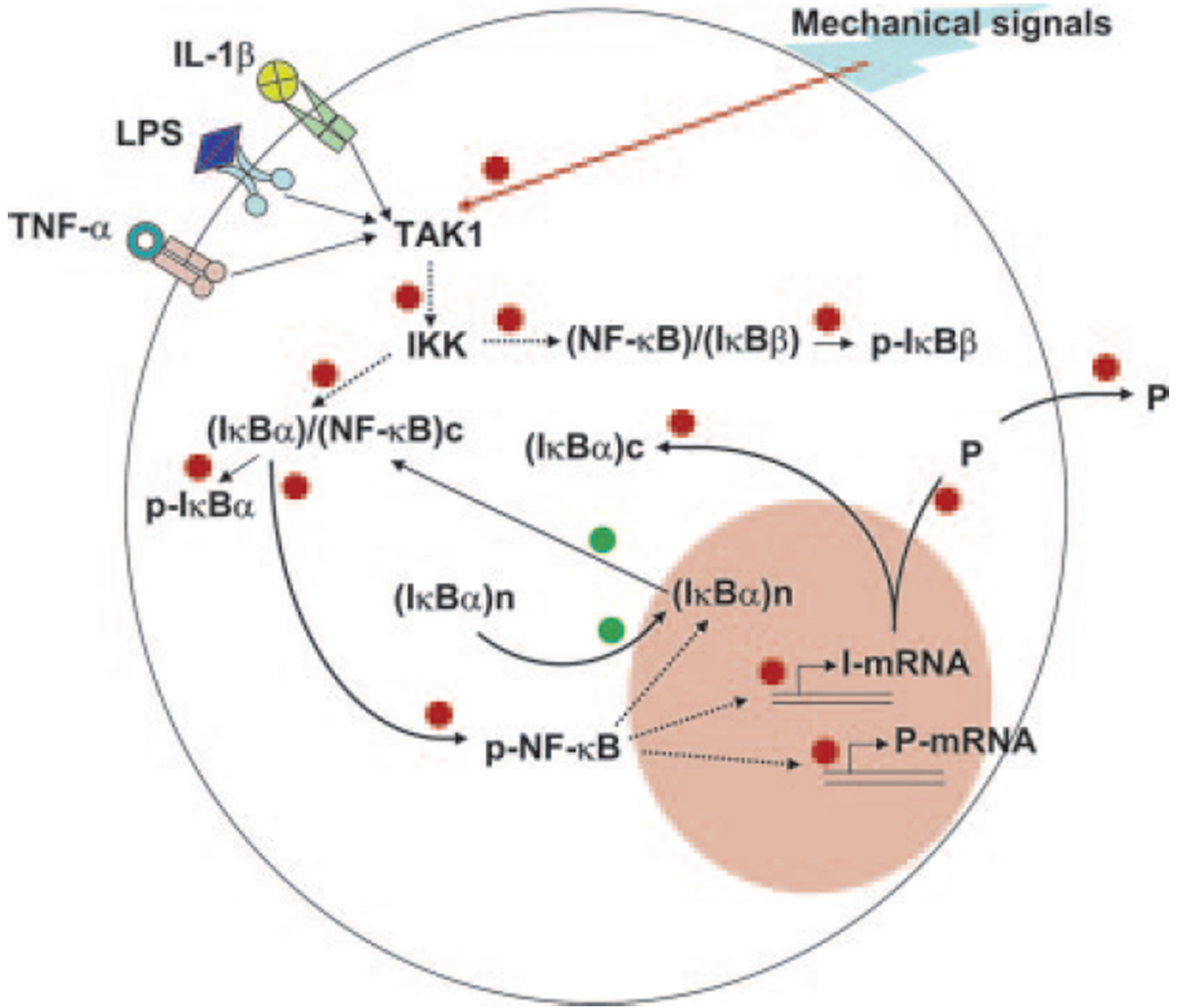


**FIGURE 5.** Schematic representation of the mechanisms of intracellular actions of CTS showing CTS suppresses IL-1β induced proinflammatory gene induction by intercepting salient steps in the NF-κB signaling cascade to inhibit its transcriptional activity by: (i) suppressing IL-1β-induced TAK1 activation and thus phosphorylation and activation of IKK. The suppression of IKK activity results in the inhibition of phosphorylation and proteosomal degradation of IκBα and IκBβ, thus inhibiting nuclear translocation of NF-κB. (ii) During the initial 30 min, CTS up-regulates IκBα nuclear translocation to prevent NF-κB binding to the DNA and facilitates export of nuclear NF-κB, that may enter the nucleus due to rapid actions of IL-1β. (iii) CTS represses IL-1β-induced IκBα and IκBβ mRNA expression to the control levels and also prevents NF-κB DNA binding. Collectively, these actions of CTS inhibit proinflammatory gene induction and molecules involved in the regulation of NF-κB signaling cascade. The red dots indicate steps within the NF-κB pathway that are inhibited

by CTS. The green dots indicate molecular events within the NF- $\kappa$ B pathway that are augmented by CTS.

Author Manuscript

Author Manuscript

Author Manuscript

Author Manuscript